LASER INTERFEROMETER GRAVITATIONAL WAVE OBSERVATORY
- LIGO -
CALIFORNIA INSTITUTE OF TECHNOLOGY
MASSACHUSETTS INSTITUTE OF TECHNOLOGY

Document Type **LIGO-T970098-01-D** Nov. 3, 1998

IO Mode Cleaner Wavefront Sensing and Control

Nergis Mavalvala

Distribution of this draft:

ISC

This is an internal working note
of the LIGO Project.

California Institute of Technology
LIGO Project - MS 51-33
Pasadena CA 91125
Phone (818) 395-2129
Fax (818) 304-9834
E-mail: info@ligo.caltech.edu

Massachusetts Institute of Technology
LIGO Project - MS 20B-145
Cambridge, MA 01239
Phone (617) 253-4824
Fax (617) 253-7014
E-mail: info@ligo.mit.edu

WWW: http://www.ligo.caltech.edu/

Introduction

The purpose of this document is to describe the wavefront sensing alignment scheme for the Input Optics Mode Cleaner (IOOMC). Sensing signals are calculated and the design of the Guoy phase telescopes is specified. The design entails calculation of the Guoy phase corresponding to maximum sensitivity to each degree of freedom and then determining the focal lengths and positions of lenses and the positions of the detectors which give this Guoy phase shift. Finally, the sensing matrix is cast into the basis of the actuators and control gains are specified.

Alignment sensitivity matrix

The mode cleaner alignment sensitivity matrix is calculated using the Modal Model [1]. A convenient basis in which the alignment degrees of freedom can be expressed is common-mode and differential tilts of the input and output mirrors. It should be noted that because the mode cleaner is a three-mirror ring cavity, the antisymmetric spatial modes of the cavity have an additional Guoy phase shift in the horizontal plane (due “spatial flips” upon reflection from the odd number of mirrors), which leads to a different Guoy phase shift for detection of horizontal and vertical misalignments. For the mode cleaner parameters listed in the Appendix, the alignment sensitivity matrix is given in Table 1:

Port	**Degree of Freedom**			
	ΔIO_x		$\overline{IO}_x$	
reflection	3.53 (3.52)		−2.25 (−2.25)	
	I (I)	90˚ (90˚)	I (I)	0˚ (0˚)
	ΔIO_y		$\overline{IO}_y$	
reflection	−2.25 (−2.25)		−1.44 (−144)	
	I (I)	0˚ (0˚)	I (I)	90˚ (90˚)

Table 1: Alignment sensitivity for the 4 km and 2 km (in parentheses) configurations. The upper entry is the signal strength per divergence angle, the lower left entry is the RF phase and the lower right entry is the Guoy phase shift for maximal detection of the signal.

Telescope layout and definitions

A schematic of the layout for the mode cleaner photodetection is given in Figure 1.

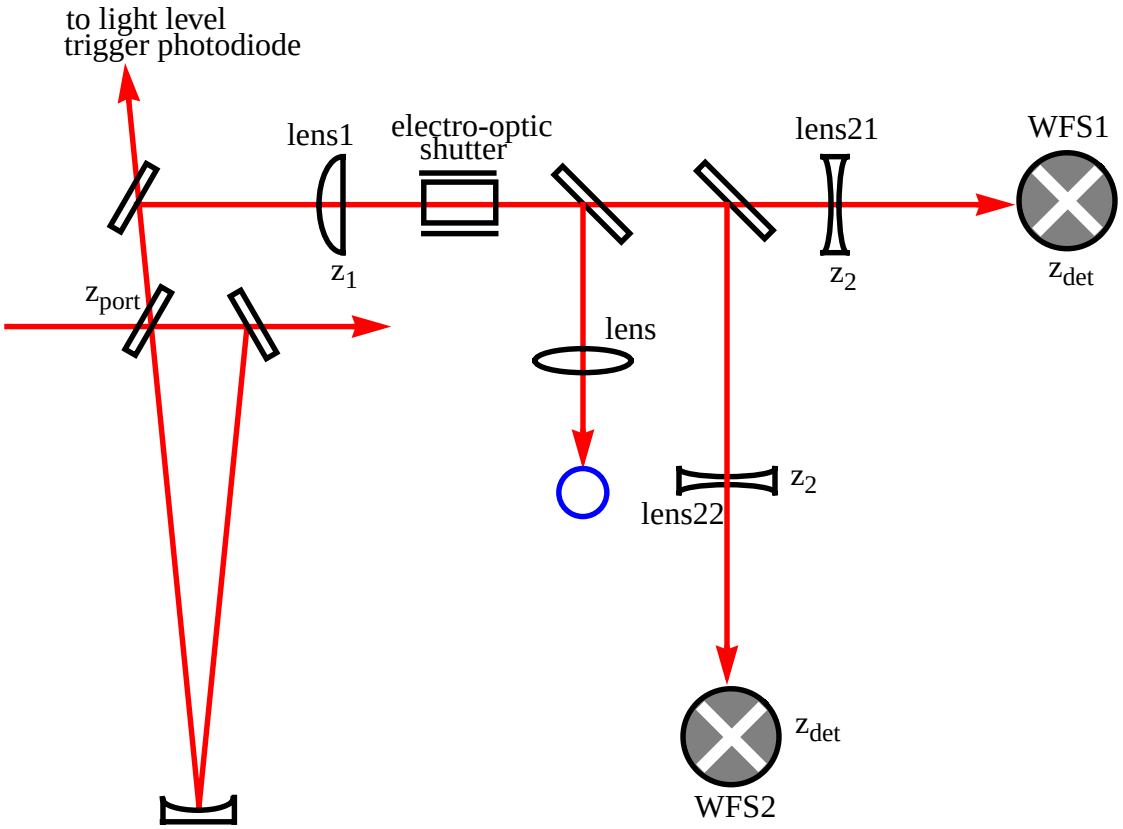

Figure 1: Schematic layout of mode cleaner photodetection. z_{port} is the location of the mode cleaner input mirror, which is also the reflection port. Since the beam waist occurs at z_{port}, we set $z = 0$ there. z_1 is the position of the first lens, with focal length, f_1; z_2 is the position of the second lens, with focal length, f_2; and z_{det} is the position of the detector.

Design constraints

The following practical considerations have driven the design choices:

- The nearest accessible position to the reflection port is about 4 m away, so $z_1 \geq 4.0$ m.
- Separation between lenses must be large enough to accommodate the electro-optic shutter and two beamsplitters, so $z_2 - z_1 \geq 0.5$ m.
- The total distance between the telescopes and the detector should not exceed 2.5 m, so $z_{det} - z_1 \leq 2.5$ m.
- The electro-optic shutter has a clear aperture of 8 mm so the spot size on it should not exceed 5 mm in diameter.
- The optimum spot size on the detector is determined by the size of the quadrant photodiodes [2]. The EG&G YAG 444-4 have an active area of 1 cm^2, which gives detector radius,

R = 5.64 mm .The ratio of the spot size on the detector, w, to the detector radius, R, which ensures that less than 1% of the signal is lost due to the finite detector size is $w/R \le 0.6$. This corresponds to $w \le 3.4$ mm . **We use w = 3.0 mm** .

- We use commercial off-the-shelf lenses; their focal lengths must be accordingly chosen.

Lens selection

To minimize spherical aberrations, we use a plano-convex lens for lens 1 and a bi-concave lens for lens 2. The CVI lenses we choose have good surface quality and figure, with a small error in the focal length. Specifically, for CVI lenses

- Surface quality: 10-5 scratch-dig (cf. 40-20 for same Newport lens)
- Surface figure: l/10 at 633 nm (cf. λ/4 to λ/2 at 546 nm for Newport)
- Focal length tolerance: ±0.5% (cf. ±2% for Newport)

The part numbers for the lenses used in the design of the Guoy phase telescopes (below) are:
CVI PLCX-25.4-515.1-C with f(1064 nm) = +1016.7 mm
CVI BICC-25.4-77.6-C with f(1064 nm) = –76.3 mm

Telescope design

The focal lengths and positions of the lenses and the position of the detector head for the Guoy phase telescopes is given in Table 2.

Detector Guoy phase	Configura-tion	f_1 (mm)	z_1 (mm)	f_2 (mm)	z_2 (mm)	z_{det} (mm)
180˚	4 km	+1016.7	4000.0	–76.3	5299.4	5637.5
90˚	4 km	+1016.7	4000.0	–76.3	4945.8	5951.7
180˚	2 km	+1016.7	4000.0	–76.3	5300.6	5595.9
90˚	2 km	+1016.7	4000.0	–76.3	4945.2	6077.4

Table 2: The Guoy phase telescopes for two wavefront sensors for the 4 km and 2 km configurations.

The Gaussian beam propagation, along with Guoy phase shift along the telescope train is give in Figure 2 for the 4 km and in Figure 3 for the 2 km configuration.

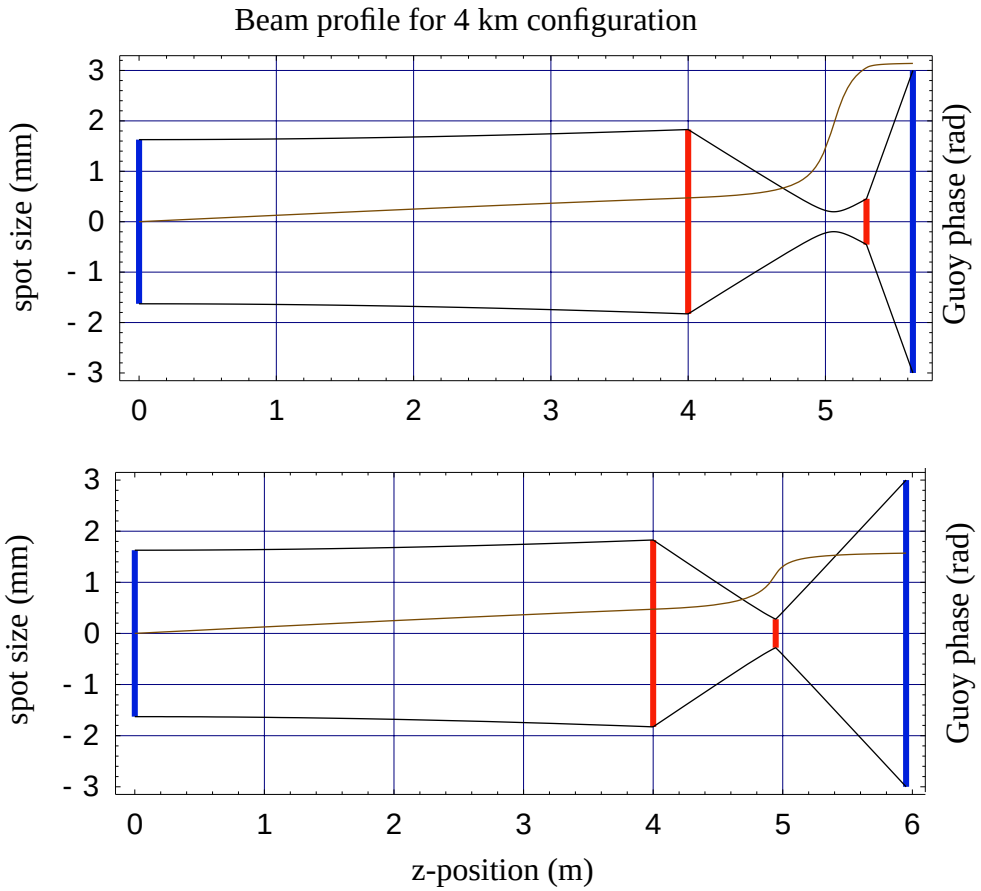

Figure 2: Beam profiles for the 4 km configuration for detectors at 0˚ (180˚) and 90˚ Guoy phase shift.

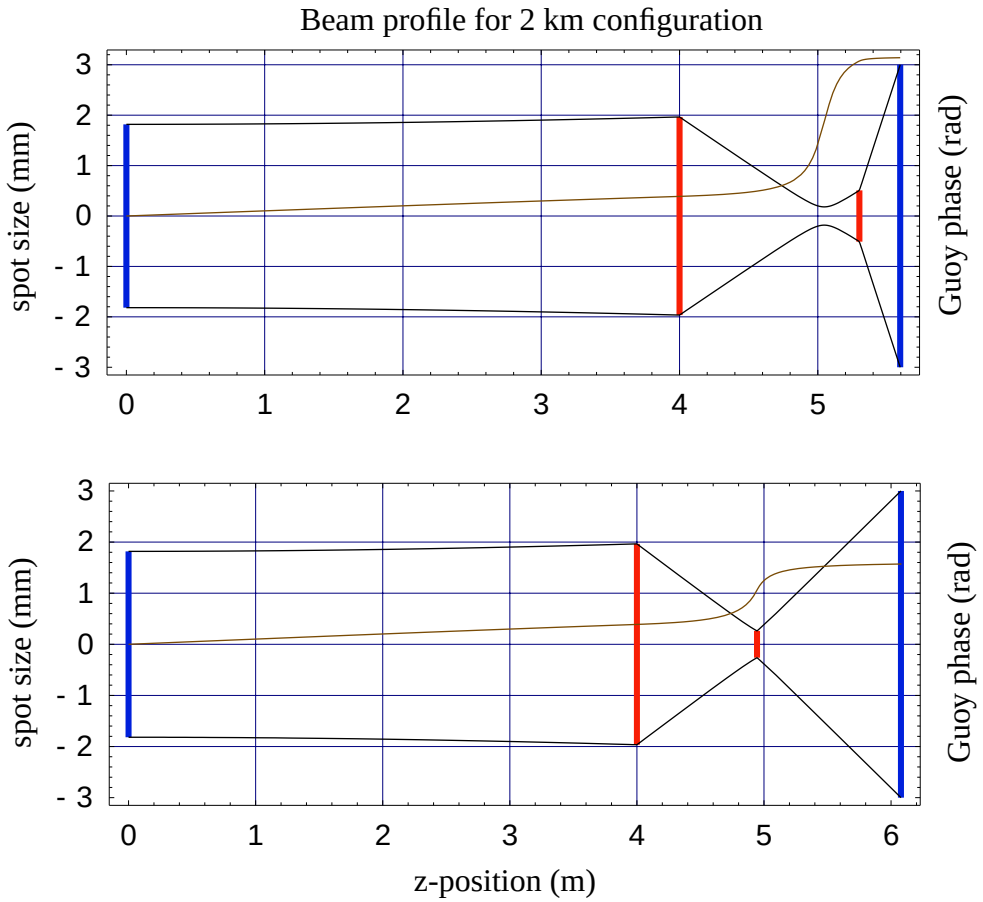

Figure 3: Beam profiles for the 2 km configuration for detectors at 0˚ (180˚) and 90˚ Guoy phase shift.

Error propagation

The dominant source of Guoy phase error in this two-lens design is error in the position of the second lens. In fact, for an error of ±10 mm in the placement of the second lens corresponds to a Guoy phase error of ±6˚ for both detectors at 90˚, and a guoy phase error of less than ±1˚ for both detectors at 0˚. All other errors contribute less than ±0.5˚ to the Guoy phase error and less than 0.1 mm to the spot size on the detector.

Control Signals

For the purposes of actuating the steering mirrors which align the input beam to the mode cleaner axes, it is more convenient to express the alignment sensing matrix given in Table 1 in terms of shifts and tilts of the input beam. The alignment sensitivity (in the horizontal plane) for the 2 km

configuration in terms of input beam shift and tilt at the mode cleaner cavity waist, Δx_{IB} and ϕ_{IB}, respectively, is

Sensor	Φ_{Guoy}	Δx_{IB}	ϕ_{IB}
WFS1x	90˚	1.59	
WFS2x	0˚		1.59

Δx_{IB} is normalized to the beam waist, w_0, while ϕ_{IB} is normalized to the beam divergence angle, θ_D. An identical matrix can be written for beam shifts and tilts in the vertical plane, Δy_{IB} and θ_{IB}, respectively.

To convert these sensor signals, A_i, into voltages at the demodulator outputs, S_i, we use

$$S_\phi \equiv S_i(\phi_{IB}) = 2J_0(\Gamma)J_1(\Gamma)P_{in}f_{split}k_{PD}^{10}\eta_{PD}Z_{PD}G_{demod}\frac{A_i(\phi_{IB})}{\phi_D}$$

and

$$S_{\Delta x} \equiv S_i(\Delta x_{IB}) = 2J_0(\Gamma)J_1(\Gamma)P_{in}f_{split}k_{PD}^{10}\eta_{PD}Z_{PD}G_{demod}\frac{A_i(\Delta x_{IB})}{w_0}$$

where

Parameter	***Value***	***Unit***	***Description***
Γ	0.1		Modulation index
P_{in}	7.5	Watt	Input power
f_{split}	0.002		Fraction of reflected light to WFS
k_{PD}^{10}	0.7		Photodiode geometrical factor
η_{PD}	0.45	Amp/Watt	Photodiode efficiency
Z_{PD}	10^3	Ω	Photodiode transimpedance
G_{demod}	8		Demodulator gain
θ_D	186	μrad	Divergence angle
w_0	1.818	mm	Beam waist

Table 3: Parameters for wavefront sensing photodetection [4].

Using the above values for the wavefront sensing photodetection, $S_\phi = 3.2 \times 10^4$ volt/radian and $S_{\Delta x} = 3.3 \times 10^3$ volt/meter. The steering mirror actuators have a tilt sensitivity of $S_{SM1} = S_{SM2} = 1.7 \times 10^{-5}$ radian/volt, which must, in turn, be converted into input beam shift and tilt at the mode cleaner cavity waist. If the distance between steering mirrors is d_1 and the

distance from second steering mirror to the mode cleaner cavity waist is d_2, then matrix which converts input beam tilts and shifts into steering mirror tilts is:

$$\begin{bmatrix} \Delta x_{IB} \\ \phi_{IB} \end{bmatrix} = \pm \begin{bmatrix} 2(d_1 + d_2) & -2d_2 \\ 2 & 2 \end{bmatrix} \begin{bmatrix} \theta_{1x} \\ \theta_{2x} \end{bmatrix}$$

An identical matrix can be written for tilts and shifts in the vertical plane. There is an uncertainty in the overall sign of the matrix, since the direction of the reflective surface of the steering mirrors was not known at the time of writing.

For the 2 km configuration, the distances d_1 and d_2 are 2.102 m and 2.572 m (2.537 m to the mode cleaner input mirror and 0.035 m from the input mirror to the mode cleaner waist), respectively. This gives the basis transformation

$$\begin{bmatrix} \Delta x_{IB} \\ \phi_{IB} \end{bmatrix} = \pm \begin{bmatrix} 8.348 & -5.144 \\ 2 & 2 \end{bmatrix} \begin{bmatrix} \theta_{1x} \\ \theta_{2x} \end{bmatrix}$$

A block diagram of the sensing system is shown in Figure 4. The control voltage to each steering

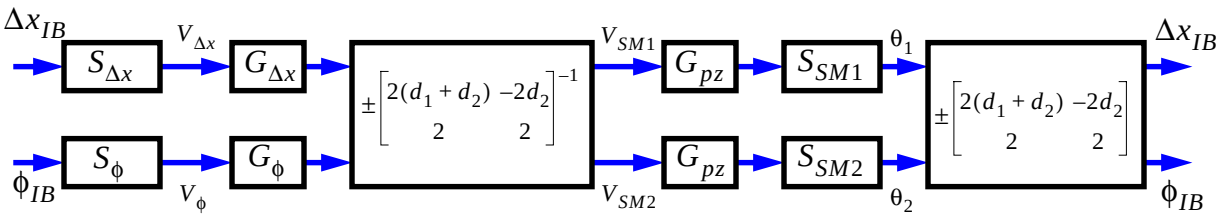

Figure 4: Block diagram of sensor and control voltages. Input beam shift and tilt are converted to sensor voltages via matrix elements, $S_{\Delta x}$ and S_ϕ; $G_{\Delta x}$ and G_ϕ are overall controller gains; multiplication by the inverse transformation matrix gives steering mirror control voltages, V_{SM1} and V_{SM2}; G_{pz} is the gain in the steering mirror PZT driver; S_{SM1} and S_{SM2} are the steering mirror sensitivities, which give steering mirror angles, θ_1 and θ_2; the transformation matrix converts these into input beam shift and tilt.

mirror is then given by the inverse transformation matrix times the overall gains of the controller, $G_{\Delta x}$ and G_ϕ. We require that the DC gain in the wavefront sensing loop is about 10. Using $G_{pz} = 15$, we get

$$\pm G_{\Delta x} \times (3.3 \times 10^3) \times (1.7 \times 10^{-5}) \times 15 \times \begin{bmatrix} 8.348 & -5.144 \\ 2 & 2 \end{bmatrix}^{-1} = 10 \Rightarrow G_{\Delta x} \approx 12$$

$$\pm G_\phi \times (3.2 \times 10^4) \times (1.7 \times 10^{-5}) \times 15 \times \begin{bmatrix} 8.348 & -5.144 \\ 2 & 2 \end{bmatrix}^{-1} = 10 \Rightarrow G_\phi \approx 1.2$$

Consequently, the voltage outputs from the controller to the steering mirror piezo driver, V_{SM1x} and V_{SM2x}, respectively, are

$$\begin{bmatrix} V_{SM1x} \\ V_{SM2x} \end{bmatrix} = \pm \begin{bmatrix} 12 & 0 \\ 0 & 1.2 \end{bmatrix} \times \begin{bmatrix} 0.074 & 0.191 \\ -0.074 & 0.309 \end{bmatrix} \begin{bmatrix} S_{\Delta x} \\ S_\phi \end{bmatrix}$$

where $S_{\Delta x}$ and S_ϕ are the wavefront sensor inputs to the controller. Again, an identical control matrix is needed for tilts/shifts in the vertical plane.

References

[1] LIGO-T960118-00-D Modal Model Update 6: Mode Cleaner (Dec. 1996).

[2] LIGO-T960111-A -D Wavefront Sensor (July 1996).

[3] LIGO-T970144-00-D Input Optics Preliminary Design (Aug. 1997).

[4] LIGO-T980064-00-D ASC Wavefront Sensing Final Design (July 1998).

Appendix

The relevant parameters for the mode cleaner for the 4 km and 2 km configuration are given in Table 4. These parameters are derived from reference [3].

Parameter	Unit	input mirror	output mirror	third mirror
length (round-trip)	m			24.510 (30.540)
power transmission		0.002	0.002	10^{-5}
power reflectivity		0.998	0.998	$1–10^{-5}$
radius of curvature	m	∞	∞	17.25 (21.50)
beam waist	mm			1.628 (1.818)
modulation frequencies	MHz			33.289 (27.717)
modulation depths	G			0.015
wave length	µm			1.064
refractive index				1.44968

Table 4: Mode cleaner parameters for the 4 km and 2 km configurations. Values for the 2 km configuration are given in parentheses, unless same for both.